www.sciencemag.org/cgi/content/full/science.aav0566/DC1

Supplementary Materials for

Aerosol-driven droplet concentrations dominate coverage and water of oceanic low-level clouds

Daniel Rosenfeld*, Yannian Zhu, Minghuai Wang*, Youtong Zheng, Tom Goren, Shaocai Yu*

*Corresponding author. Email: daniel.rosenfeld@huji.ac.il (D.R.); minghuai.wang@nju.edu.cn (M.W.); shaocaiyu@zju.edu.cn (S.Y.)

Published 17 January 2019 on *Science* First Release
DOI: 10.1126/science.aav0566

This PDF file includes:

Supplementary Text

Satellite-based estimation of cloud-top radiative cooling rate

We calculate the CTRC by running the Santa Barbara DISORT Atmospheric Radiative Transfer (SBDART) model. The input data come from two sources: MODIS-derived cloud properties and reanalysis sounding from NCEP reanalysis. The satellite-retrieved cloud quantities include the CTT, CTH, CBH, τ, and r_e. We use CTT and CTH to revise the reanalysis temperature/moisture sounding. By assuming a relative humidity of 100% at the cloud top, we can compute the cloud-top water vapor density with the retrieved CTT. The in-cloud temperature and moisture soundings are adjusted assuming moist adiabatic profile. The cloud-base values, in combination with the reanalysis temperature and moisture at 2 m above the surface level, were then used to constrain the sub-cloud layer soundings. Then we assume an inversion-layer depth of 200 m and adjust the above-cloud soundings accordingly. Figure S13 shows an example illustrating the revision of raw reanalysis soundings and how the revised soundings are compared with the radiosonde measurements. The case was on 21 July, 2013, selected during the Marine ARM (Atmospheric Radiation Measurement) GPCI (Global Energy and Water Cycle Experiment-Cloud System Study-Pacific Cross-section Inter-comparison) Investigation of Clouds (MAGIC) field campaign. The upper and bottom panel represent the radiosonde and reanalysis data, respectively. From the Fig. S13d and e, the revision (solid lines) markedly improves the original reanalysis sounding (dashed lines) as seen from the much better agreement with the radiosonde sounding (Fig. 13a and b). As a result, the estimated CTRC from the revised reanalysis agrees well with the "ground truth" calculation (Fig. 13c and f) for this case. A systematic comparison between satellite-estimated CTRC and the "ground truth" measurements for a total of 58 cases during the MAGIC campaign shows a correlation coefficient of 0.91 with 13% error (*35*). Such a good performance of this satellite estimation largely benefits from the fact that the CTRC is mostly sensitive to cloud-top properties and the free-tropospheric sounding, both of which are well constrained by satellite data.

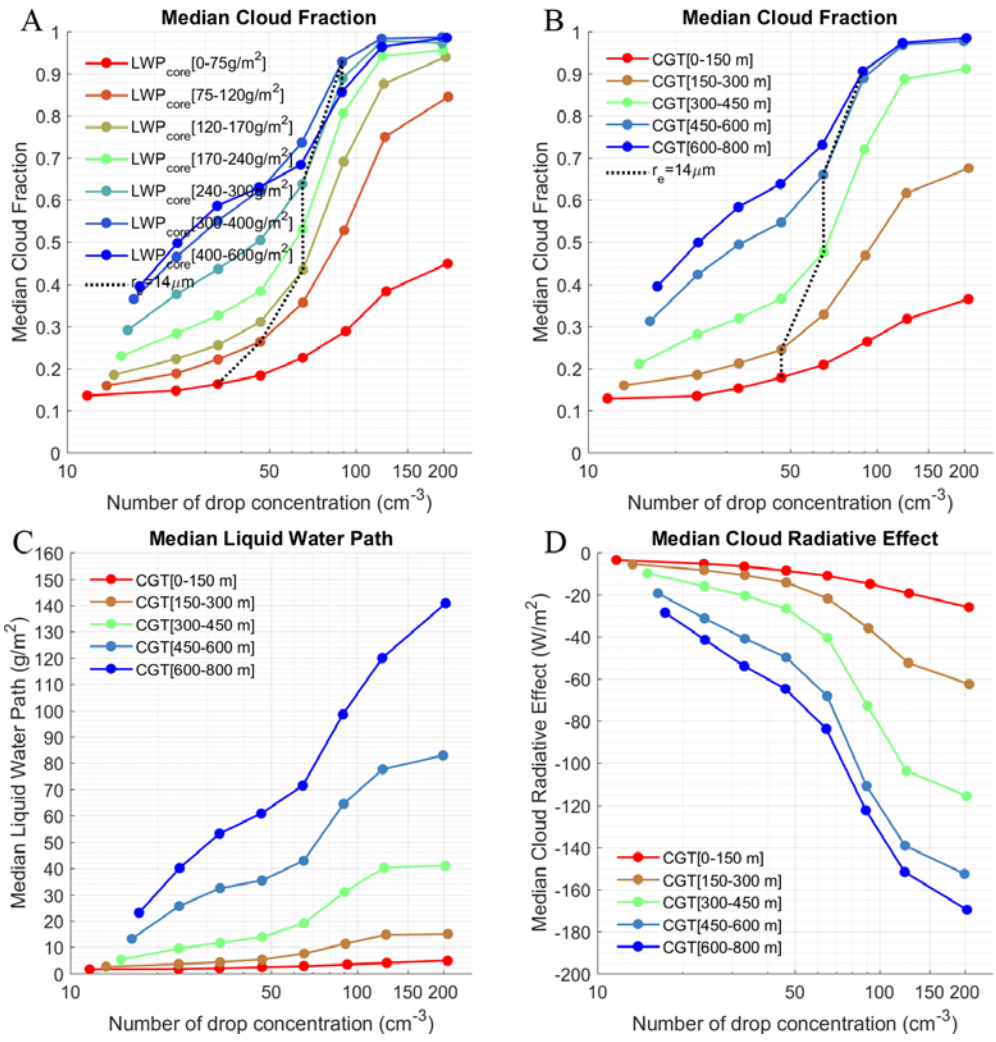

Fig. S1. Same as Fig. 3, but for the mean instead of the median values for each bin.

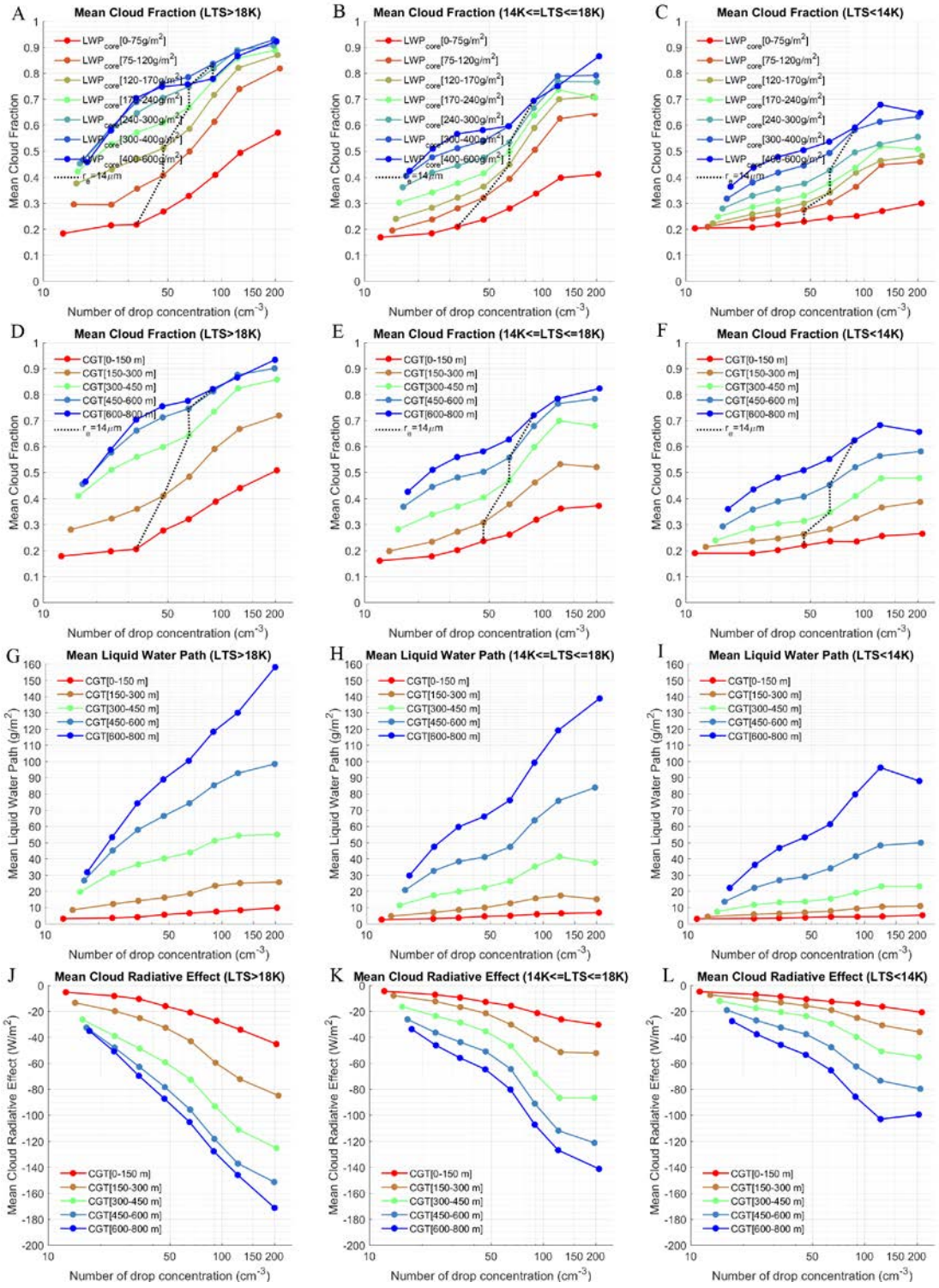

Fig. S2. Same as Fig. S1, but for LTS >18K (A,D,G,J), 14K⩽LTS⩽18K (B,E,H,K), and LTS<14K (C,F,I,L).

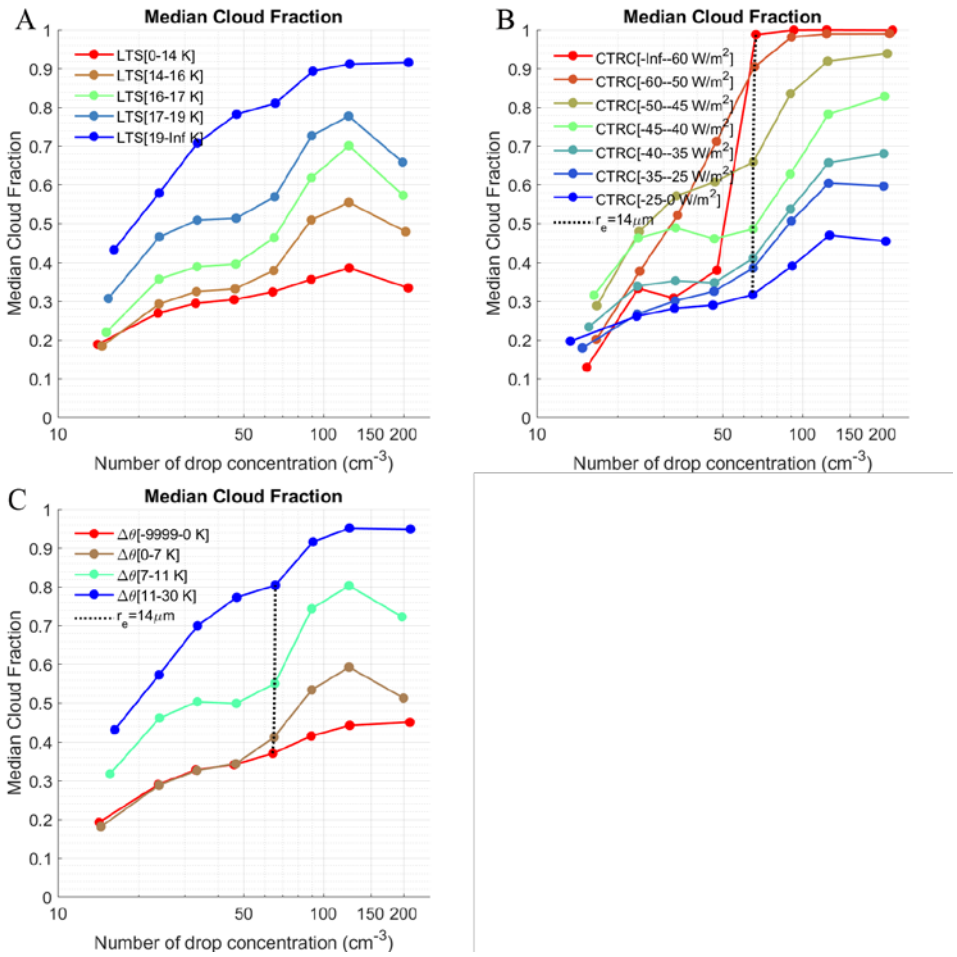

Fig. S3. The dependence of median Cf on Nd for intervals of (A) low tropospheric static stability; (B) cloud top radiative cooling rate, and (C) Inversion strength at cloud tops, Δθ; Cloud top drop effective radius of each line (i.e., for a given LWP) decreases with increasing drop concentrations, and reaches 14 μm at the broken line. The box plot distributions for each bin are shown in Figures S8-S10.

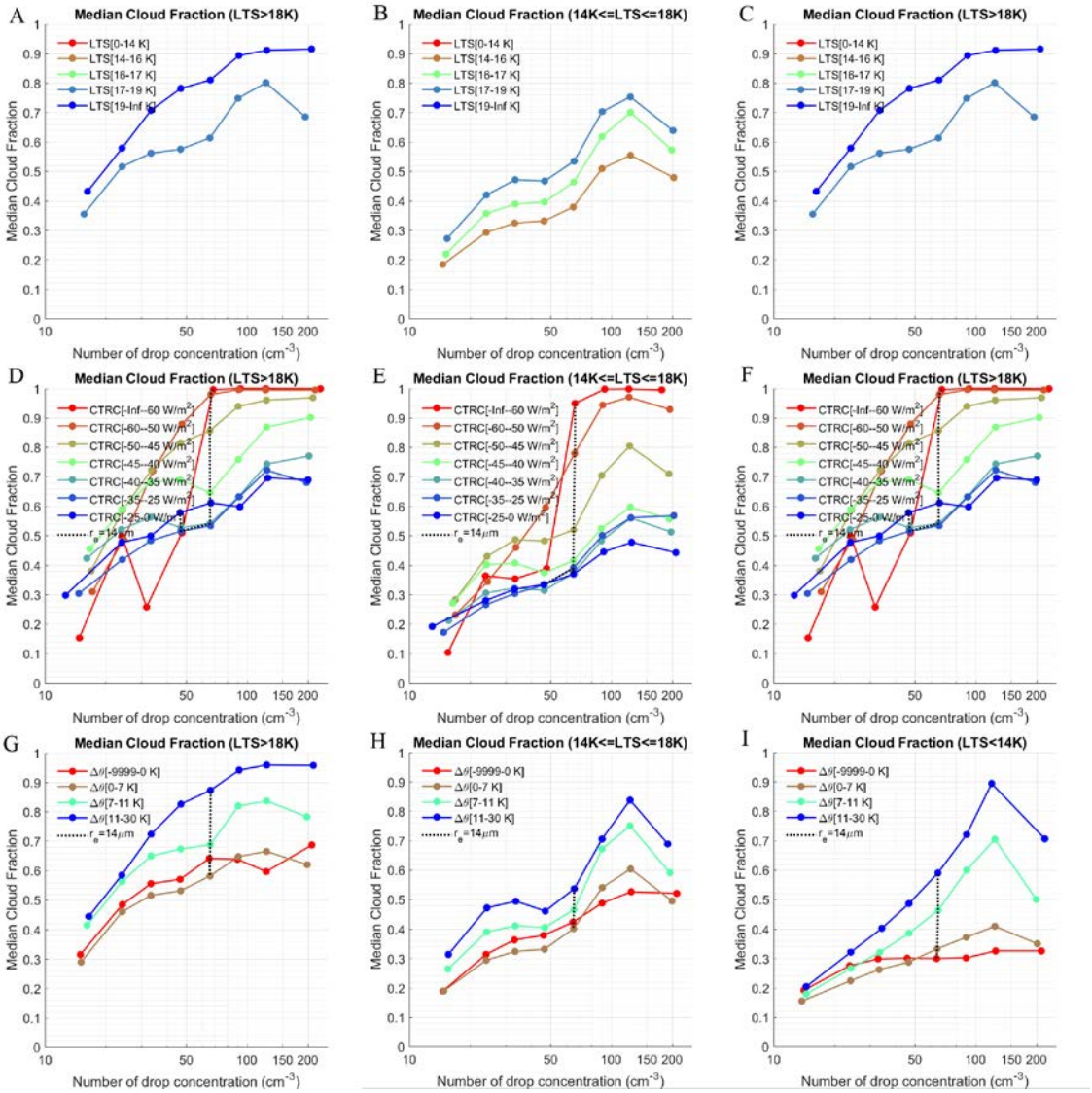

Fig. S4. Same as Fig. S3, but for LTS >18K (A,D,G), 14K≤LTS≤18K (B,E,H), and LTS<14K (C,F,I).

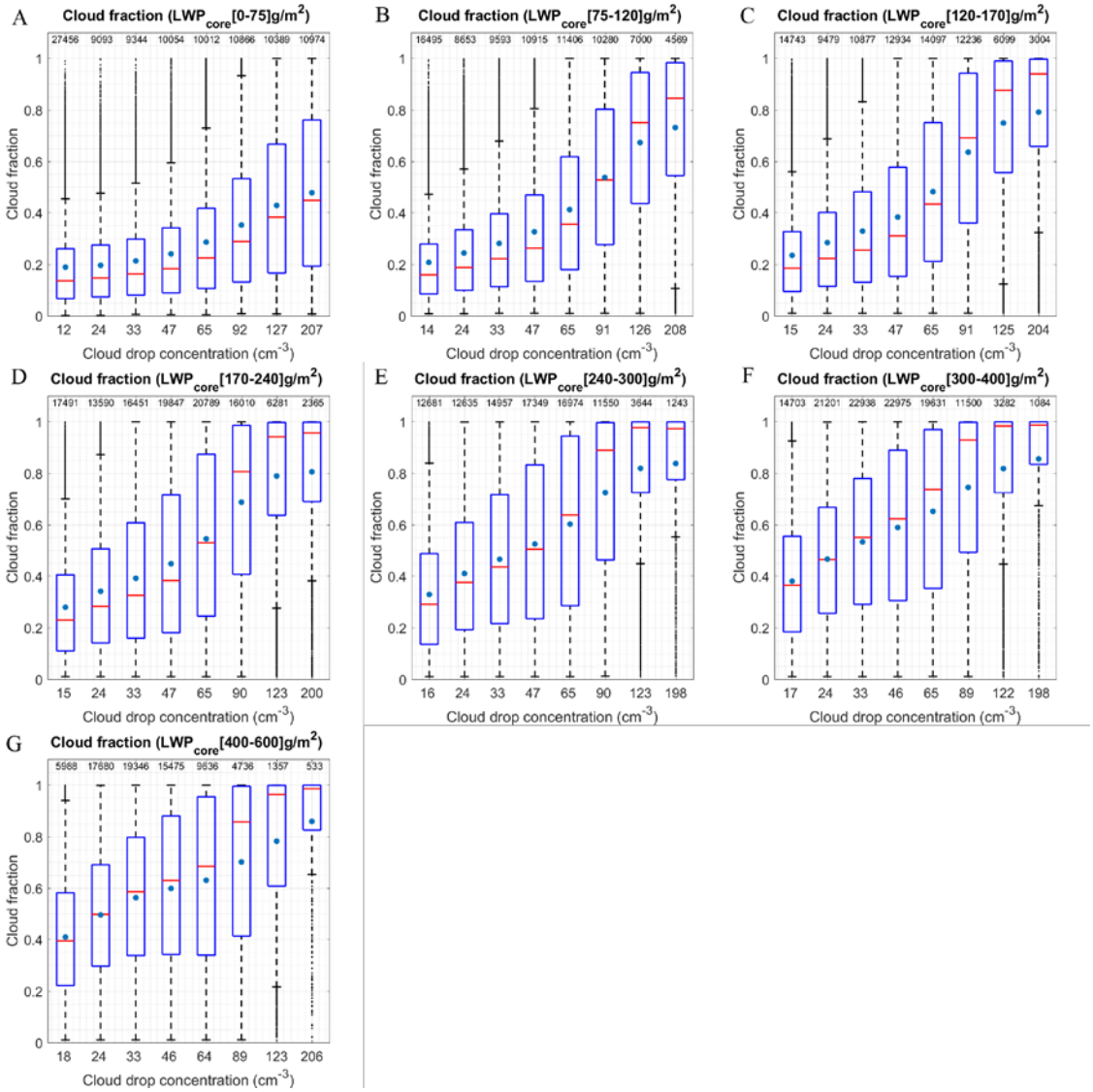

Fig. S5. The cloud fraction as a function of N_d bins for different LWP_{core} intervals. The box plot distributions and number of cases that their median constitute each of the points that compose Fig. 1A. The horizontal bars are the medians and the dots are the means. The number of 1x1 degree areas composing each distribution are given at the top.

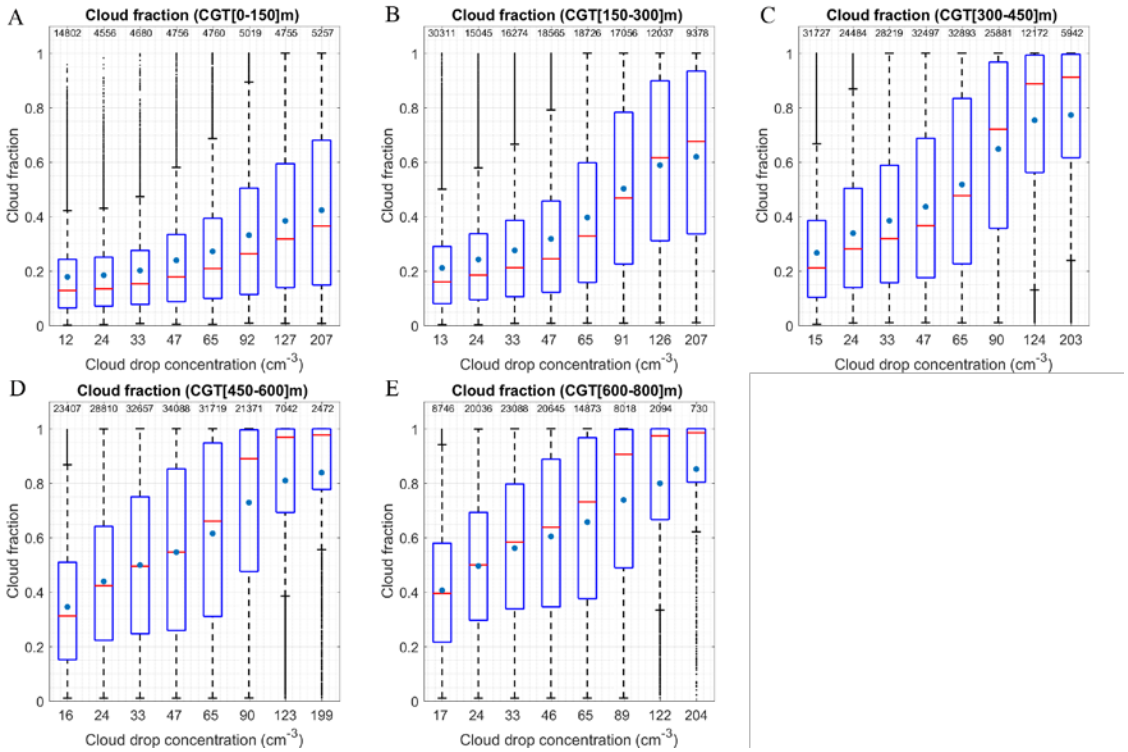

Fig. S6. The cloud fraction as a function of N_d bins for different CGT intervals. The box plot distributions and number of cases that their median constitute each of the points that compose Fig. 1B. The horizontal bars are the medians and the dots are the means. The number of 1x1 degree areas composing each distribution are given at the top.

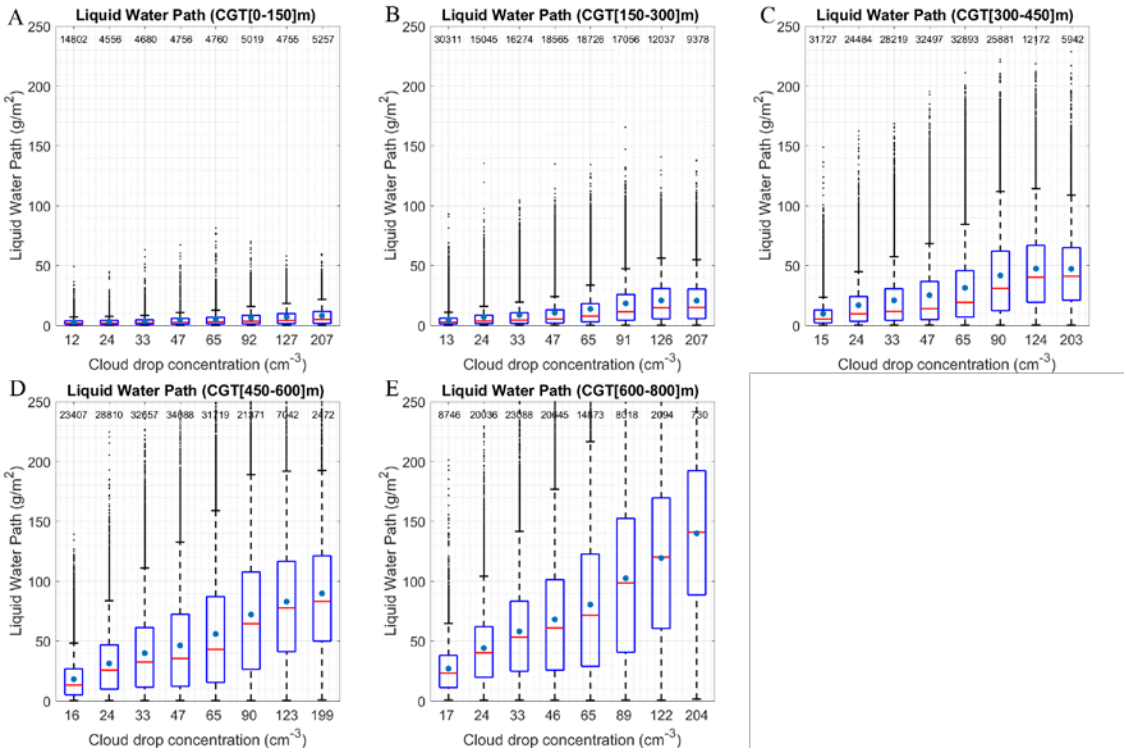

Fig. S7. The LWP as a function of N_d bins for different CGT intervals. The box plot distributions and number of cases that their median constitute each of the points that compose Fig. 1C. The horizontal bars are the medians and the dots are the means. The number of 1x1 degree areas composing each distribution are given at the top.

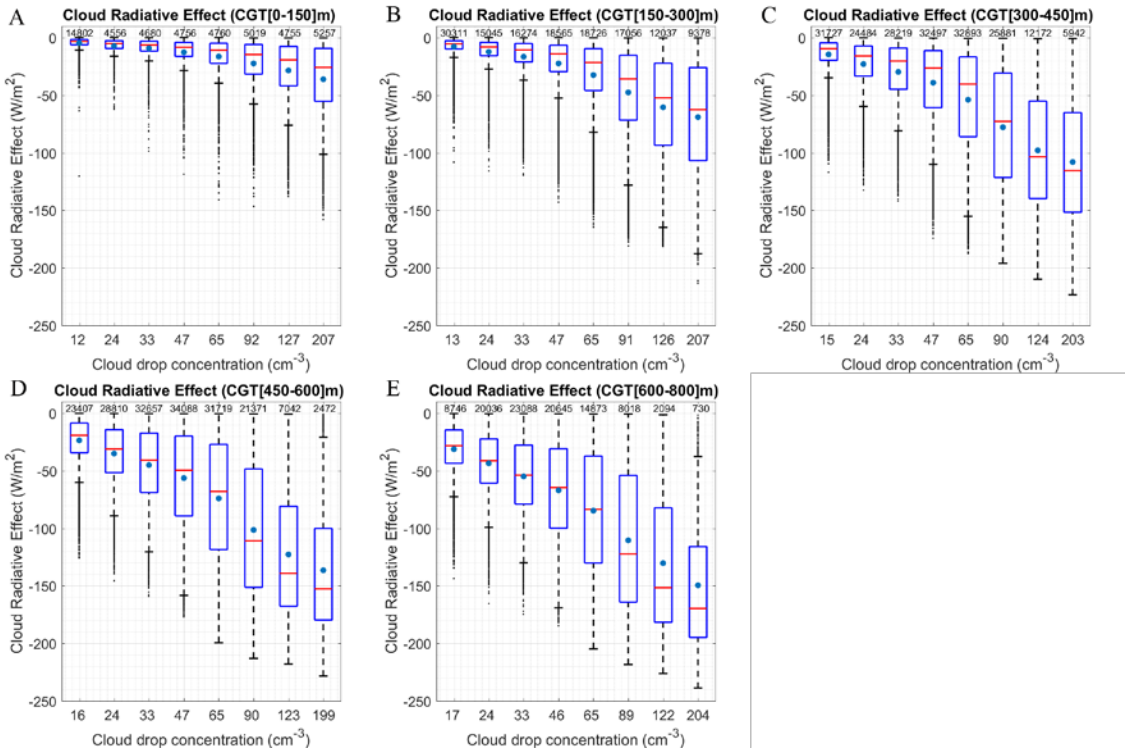

Fig. S8. The CRE as a function of N_d bins for different CGT intervals. The box plot distributions and number of cases that their median constitute each of the points that compose Fig. 1D. The horizontal bars are the medians and the dots are the means. The number of 1x1 degree areas composing each distribution are given at the top.

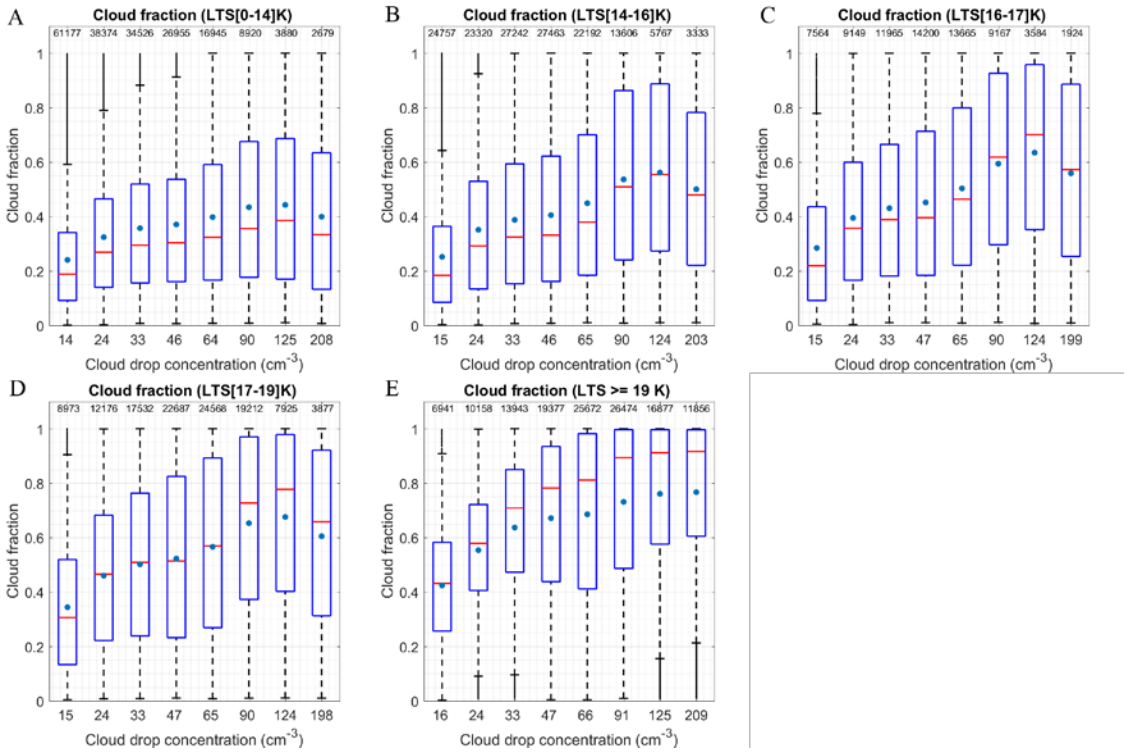

Fig. S9. The cloud fraction as a function of N_d bins for different LTS intervals. The box plot distributions and number of cases that their median constitute each of the points that compose Fig. S2A. The horizontal bars are the medians and the dots are the means. The number of 1x1 degree areas composing each distribution are given at the top.

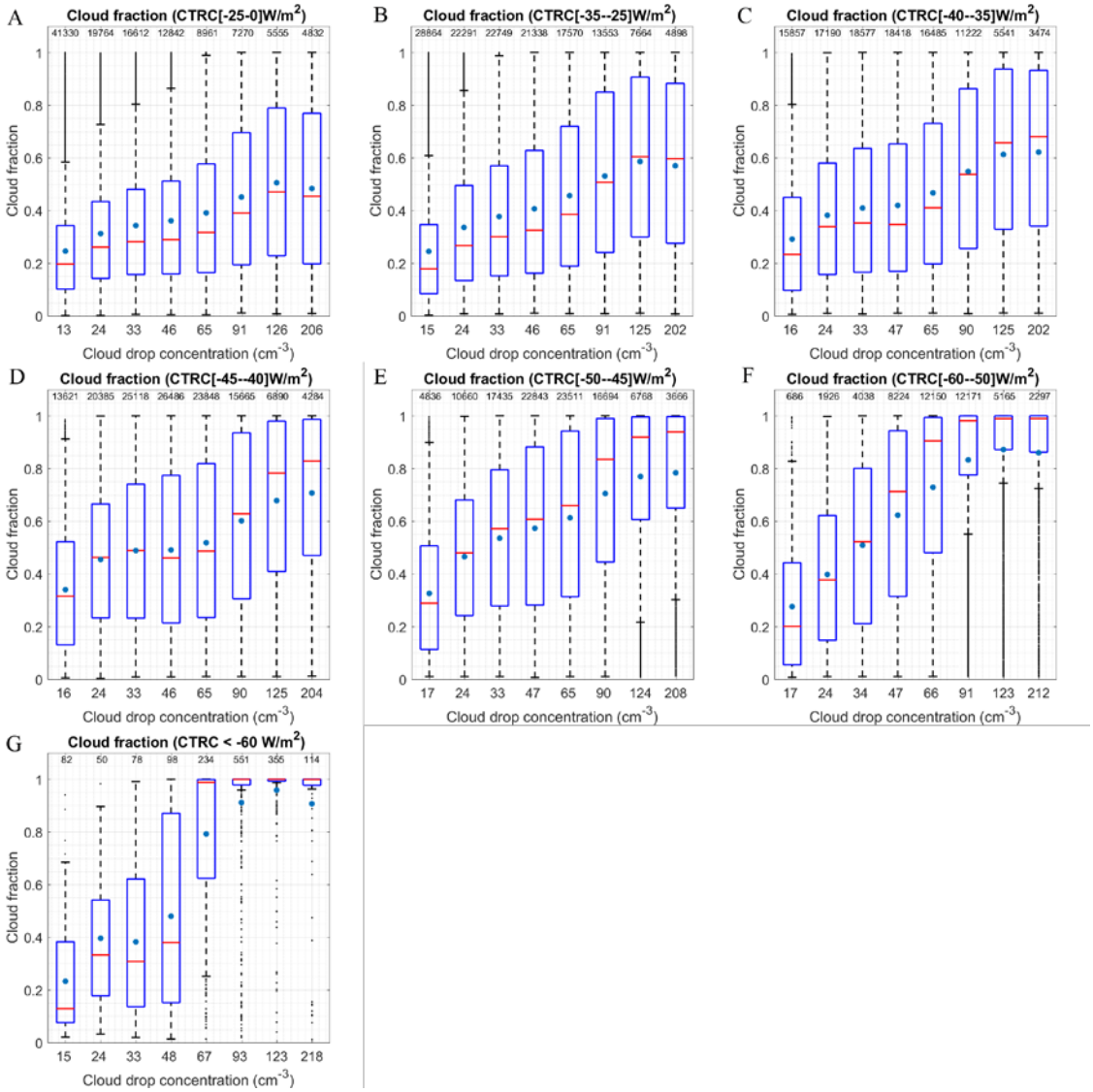

Fig. S10. The cloud fraction as a function of N_d bins for different CTRC intervals. The box plot distributions and number of cases that their median constitute each of the points that compose Fig. S2B. The horizontal bars are the medians and the dots are the means. The number of 1x1 degree areas composing each distribution are given at the top.

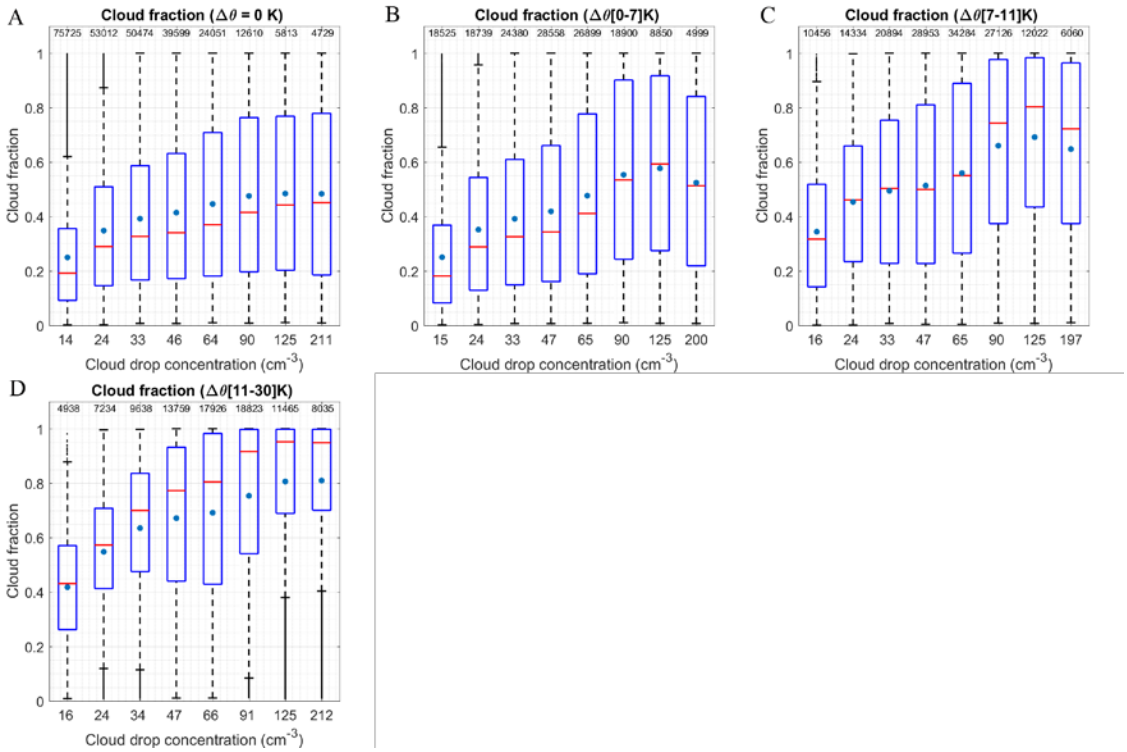

Fig. S11. The cloud fraction as a function of N_d bins for different Δθ intervals. The box plot distributions and number of cases that their median constitute each of the points that compose Fig. S2C. The horizontal bars are the medians and the dots are the means. The number of 1x1 degree areas composing each distribution are given at the top.

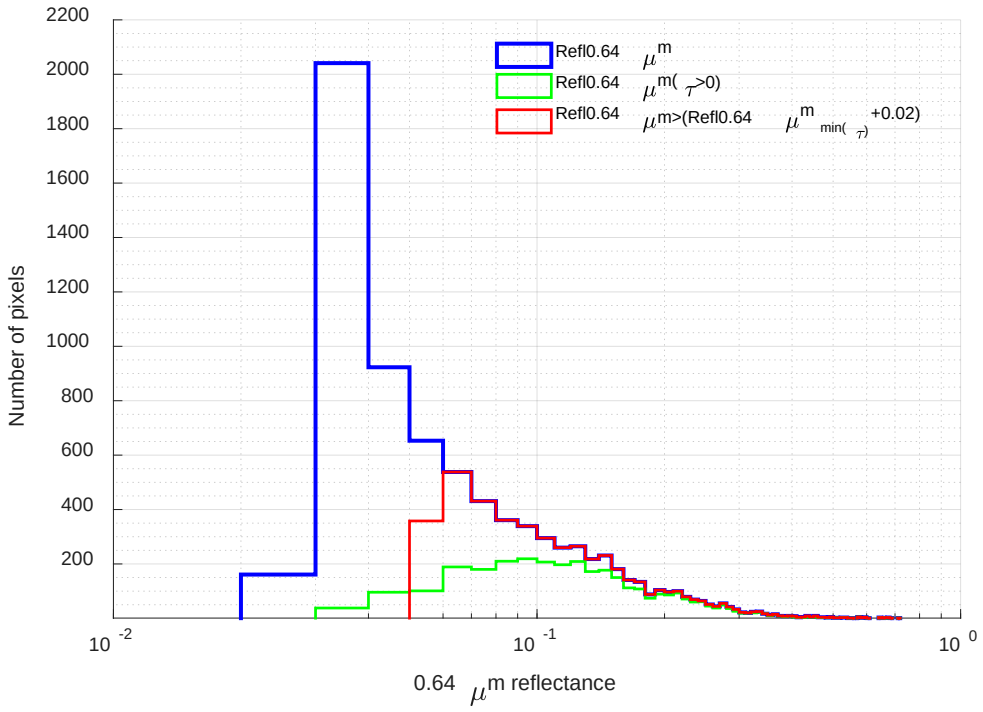

Fig. S12. Demonstration of the cloud fraction calculation for a given scene (Feb 19th, 2015, center at Latitude:-0.43°, Longitude:-169.18°). The green line represented the histogram of reflectance at 0.64 μm where has τ>0. Similarly, the red line represents the histogram of the pixels have 0.64 μm reflectance

greater than the reflectance that is matched to the minimum detectable τ. For this case, the calculated Cf are 0.40 and 0.59 for green and red lines respectively.

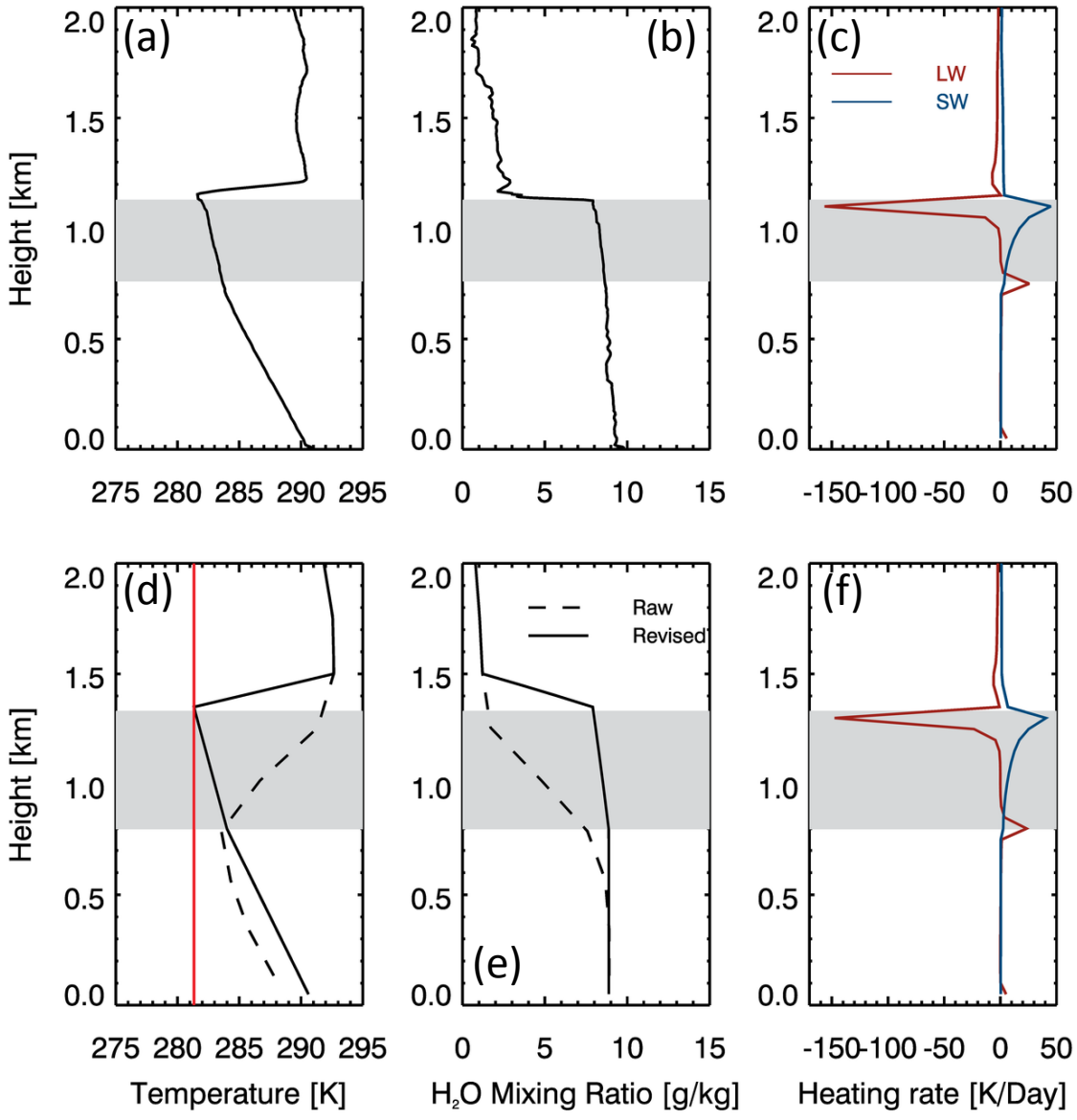

Figure S13: Profiles of temperature (a, d), water vapor mixing ratio (b, e), and heating rate (c,f) from radiosonde (upper panel) and reanalysis (bottom panel). In d, the vertical red line marks the satellite-retrieved cloud top temperature. The solid and dashed lines represent the revised and raw reanalysis sounding.

Table S1. Same as Table 2, but for N_d. Multiple regression with polynomial fit of the second order for Cf with $Log_{10}(N_d)$, $\Delta\theta$ and CTRC for different intervals of CGT. The values in the 3 right columns are the partial R^2, or fraction of explained variability of Cf by N_d, $\Delta\theta$ and CTRC. Note that N_d explains nearly 3/4 of the variability in CRE for a given CGT, as shown in Fig. 3D.Table S2.

CGT [m]	**Total R^2**	**RMS Error**	**log (N_d)**	**$\Delta\theta$**	**CTRC**
Cf		**[-]**		**K**	**Wm^{-2}**
0-150	0.932	0.035	0.719	0.163	0.050
150-300	0.910	0.061	0.657	0.127	0.126
300-450	0.925	0.055	0.629	0.160	0.136
450-600	0.899	0.060	0.647	0.169	0.082
600-800	0.873	0.060	0.623	0.145	0.105
LWP		**[g m^{-2}]**			
0-150	0.852	1.259	0.527	0.236	0.089
150-300	0.865	4.390	0.283	0.173	0.408
300-450	0.886	6.480	0.319	0.221	0.346
450-600	0.867	10.841	0.546	0.124	0.197
600-800	0.897	13.122	0.682	0.041	0.174
CRE		**[wm^{-2}]**			
0-150	0.943	3.468	0.763	0.149	0.030
150-300	0.922	8.797	0.592	0.107	0.224
300-450	0.943	9.167	0.650	0.110	0.183
450-600	0.928	11.684	0.734	0.085	0.110
600-800	0.936	11.148	0.764	0.052	0.120

Table S2.

Table S2.1, Coefficients of multiple regression with polynomial fit of the second order for Cf with $\log_{10}(N_d)$, LTS and CTRC

	Coefficients		
	Cf	$LWP_{average}$	CRE
CGT^2	-6.74013E-01	1.76970E-04	3.66454E-05
$CGT \times \log_{10}(N_d)$	5.50474E-05	1.44208E-01	-1.20699E-01
CGT×LTS	1.89463E-05	9.41140E-03	-6.08122E-03
CGT×CTRC	-1.15019E-06	2.88727E-04	1.17351E-04
CGT	7.45851E-04	-3.87350E-01	1.65038E-01
$\log_{10}(N_d)^2$	2.11680E-02	-3.50530E+00	-2.04209E+01
$\log_{10}(N_d) \times$LTS	8.42938E-03	2.12819E+00	-3.99771E+00
$\log_{10}(N_d) \times$CTRC	-9.01241E-03	-4.70276E-01	1.14618E+00
$\log_{10}(N_d)$	-2.31617E-01	-5.72627E+01	1.56830E+02
LTS^2	-6.86324E-04	-1.52631E-01	1.31675E-01
LTS×CTRC	4.49587E-04	6.90503E-02	-5.64969E-02
LTS	4.46546E-02	3.49598E+00	-1.01558E+00
$CTRC^2$	2.02720E-04	4.41370E-02	-4.23289E-02
CTRC	2.30734E-02	2.65287E+00	-3.84016E+00
constant	-5.32511E-02	8.08247E+01	-1.55510E+02

Table S2.2 Coefficients of multiple regression with polynomial fit of the second order for Cf with $\log_{10}(N_d)$, $\Delta\theta$ and CTRC

	Coefficients		
	Cf	$LWP_{average}$	CRE
CGT^2	-7.10431E-07	1.31485E-04	6.17390E-05
$CGT \times \log_{10}(N_d)$	1.46158E-04	1.57701E-01	-1.33537E-01
$CGT \times \Delta\theta$	1.31106E-06	1.99350E-03	-1.50789E-03
CGT×CTRC	-5.45026E-06	-1.56801E-03	1.10417E-03
CGT	6.97372E-04	-3.17076E-01	1.24522E-01
$\log_{10}(N_d)^2$	4.01239E-02	6.90955E-01	-2.56514E+01
$\log_{10}(N_d) \times \Delta\theta$	9.51925E-03	7.82047E-01	-2.58789E+00
$\log_{10}(N_d) \times$CTRC	-5.32763E-03	-2.92653E-01	8.44217E-01
$\log_{10}(N_d)$	-8.35930E-02	-3.50551E+01	1.12136E+02
$\Delta\theta^2$	8.74063E-05	1.76373E-02	-2.51274E-02
$\Delta\theta \times$CTRC	-3.49189E-04	-6.54616E-02	7.15781E-02
$\Delta\theta$	-1.83496E-02	-3.84826E+00	6.47132E+00
$CTRC^2$	5.66640E-05	9.71324E-03	-1.11179E-02
CTRC	1.59196E-02	1.73881E+00	-2.55785E+00
constant	2.71063E-01	8.96093E+01	-1.34376E+02

Table S2.3 Coefficients of multiple regression with polynomial fit of the second order for Cf with $\log_{10}(N_d/W_b^{0.5})$, and CTRC

	Coefficients		
	Cf	$LWP_{average}$	CRE
CGT^2	-4.95543E-07	1.41445E-04	2.11668E-05
$CGT\times\log_{10}(N_d/W_b^{0.5})$	1.91532E-04	1.47582E-01	-1.22848E-01
CGT×LTS	2.31120E-05	8.24980E-03	-5.25877E-03
CGT×CTRC	-1.56665E-06	5.82819E-04	-1.18194E-04
CGT	2.62163E-04	-3.68739E-01	1.84456E-01
$\log_{10}(N_d/W_b^{0.5})^2$	6.46651E-02	-9.96660E-01	-3.08719E+01
$\log_{10}(N_d/W_b^{0.5})\times$LTS	1.50697E-02	3.25238E+00	-4.51614E+00
$\log_{10}(N_d/W_b^{0.5})\times$CTRC	-8.24803E-03	-2.78810E-01	8.43776E-01
$\log_{10}(N_d/W_b^{0.5})$	-5.24256E-01	-7.84239E+01	2.02349E+02
LTS^2	-1.45163E-04	-1.20300E-01	8.17321E-02
LTS×CTRC	5.15651E-04	8.19169E-02	-6.64008E-02
LTS	1.33540E-02	8.21935E-01	1.78916E+00
$CTRC^2$	1.84189E-04	4.55344E-02	-3.96966E-02
CTRC	2.11852E-02	2.15325E+00	-3.03469E+00
constant	4.91849E-01	1.12229E+02	-2.16206E+02

Table S2.4 Coefficients of multiple regression with polynomial fit of the second order for Cf with $\log_{10}(N_d/W_b^{0.5})$, $\Delta\theta$ and CTRC

	Coefficients		
	Cf	LWP_average	CRE
CGT^2	-5.20412E-07	8.94761E-05	4.62832E-05
$CGT\times\log_{10}(N_d/W_b^{0.5})$	2.63277E-04	1.51284E-01	-1.26869E-01
$CGT\times\Delta\theta$	6.28499E-06	1.55349E-03	-1.24522E-03
CGT×CTRC	-6.23672E-06	-1.52396E-03	1.11880E-03
CGT	2.45838E-04	-3.05552E-01	1.52230E-01
$\log_{10}(N_d/W_b^{0.5})^2$	1.21903E-01	8.63985E+00	-4.11349E+01
$\log_{10}(N_d/W_b^{0.5})\times\Delta\theta$	9.31700E-03	8.91438E-01	-2.17551E+00
$\log_{10}(N_d/W_b^{0.5})\times$CTRC	-6.19273E-03	-4.57559E-01	8.50075E-01
$\log_{10}(N_d/W_b^{0.5})$	-4.60532E-01	-6.86739E+01	1.75006E+02
$\Delta\theta^2$	1.47450E-04	1.83971E-02	-2.61888E-02
$\Delta\theta\times$CTRC	-3.02845E-04	-5.94642E-02	6.26179E-02
$\Delta\theta$	-2.14331E-02	-3.89954E+00	5.92309E+00
$CTRC^2$	3.25041E-05	5.66408E-03	-4.72092E-03
CTRC	1.67688E-02	1.71821E+00	-2.17631E+00
constant	6.61140E-01	1.17774E+02	-1.90085E+02

Table S3. Coefficients of multiple regression with polynomial fit of the second order for Cf, LWP and CRE with $Log_{10}(N_d/W_b^{0.5})$, LTS and CTRC for different intervals of CGT.

	Coefficients				
	Cf				
CGT[m]	0-150	150-300	300-450	450-600	600-800
$\log_{10}(N_d/W_b^{0.5})^2$	1.18714E-01	1.55303E-01	5.69580E-02	-1.15867E-01	-2.11737E-01
$\log_{10}(N_d/W_b^{0.5})\times$LTS	1.76865E-02	1.53946E-02	9.48784E-03	1.28244E-02	1.80381E-02
$\log_{10}(N_d/W_b^{0.5})\times$CTRC	-5.07513E-03	-9.17625E-03	-9.51958E-03	-9.04303E-03	-8.02936E-03
$\log_{10}(N_d/W_b^{0.5})$	-6.66649E-01	-8.11120E-01	-3.55468E-01	2.32741E-01	5.46725E-01
LTS^2	5.80331E-04	8.85080E-04	1.96935E-05	-1.13677E-04	-6.55903E-04
LTS×CTRC	2.21470E-04	1.61253E-04	2.37620E-04	9.47426E-04	1.24853E-03
LTS	-3.38613E-02	-2.91508E-02	2.64914E-02	4.93126E-02	5.96270E-02
$CTRC^2$	7.27014E-06	9.80262E-05	1.77930E-04	2.94522E-04	2.62931E-04
CTRC	8.56704E-03	2.16460E-02	2.65834E-02	2.26063E-02	1.40227E-02
constant	9.87006E-01	1.18011E+00	3.99762E-01	-2.93046E-01	-6.77496E-01
	LWP				
CGT[m]	0-150	150-300	300-450	450-600	600-800
$\log_{10}(N_d/W_b^{0.5})^2$	1.59374E+00	2.57911E+00	-5.51389E+00	-1.53407E+01	-2.49188E+01
$\log_{10}(N_d/W_b^{0.5})\times$LTS	4.22581E-01	1.04312E+00	2.47008E+00	4.33802E+00	5.71783E+00
$\log_{10}(N_d/W_b^{0.5})\times$CTRC	-7.79838E-02	-3.79837E-01	-3.78152E-01	-5.38516E-01	-1.14255E+00
$\log_{10}(N_d/W_b^{0.5})$	-1.06518E+01	-2.73718E+01	-8.34143E+00	1.51644E+01	4.05042E+01
LTS^2	1.48647E-02	4.72932E-02	-7.81423E-03	-6.90974E-03	-2.28862E-01
LTS×CTRC	5.85299E-03	-9.24063E-03	-2.49655E-02	1.03447E-01	3.89293E-01
LTS	-7.77659E-01	-2.53620E+00	-2.04041E+00	4.09783E-01	1.64870E+01
$CTRC^2$	1.40988E-03	1.39656E-02	2.96282E-02	6.70806E-02	1.09061E-01
CTRC	2.07298E-01	1.70635E+00	3.02007E+00	3.94883E+00	4.09623E+00
constant	1.76598E+01	6.06260E+01	4.83449E+01	7.54761E+00	-1.48116E+02
	CRE				
CGT[m]	0-150	150-300	300-450	450-600	600-800
$\log_{10}(N_d/W_b^{0.5})^2$	-1.68639E+01	-3.41280E+01	-4.11857E+01	-3.82838E+01	-3.28584E+01
$\log_{10}(N_d/W_b^{0.5})\times$LTS	-1.91048E+00	-3.36296E+00	-4.69972E+00	-5.29494E+00	-5.76827E+00
$\log_{10}(N_d/W_b^{0.5})\times$CTRC	1.87786E-01	9.48032E-01	1.03298E+00	1.27209E+00	1.66873E+00
$\log_{10}(N_d/W_b^{0.5})$	7.62432E+01	1.69323E+02	2.01783E+02	1.95592E+02	1.88830E+02
LTS^2	-2.73027E-02	-5.18022E-02	4.61020E-02	2.26296E-02	1.71663E-01
LTS×CTRC	-1.14846E-02	1.24795E-02	5.36856E-03	-1.31197E-01	-2.62325E-01
LTS	3.20229E+00	5.91427E+00	2.88859E+00	-6.54896E-01	-8.77226E+00
$CTRC^2$	-5.55033E-04	-1.94330E-02	-3.17978E-02	-6.04180E-02	-7.02555E-02
CTRC	-2.57491E-01	-3.00791E+00	-3.90748E+00	-4.26488E+00	-3.90019E+00
constant	-8.43720E+01	-2.09835E+02	-2.12928E+02	-1.81375E+02	-1.18694E+02